

IDENTIFICATION OF THE DYNAMIC PROPERTIES OF NONLINEAR VICOELASTIC MATERIALS AND THE ASSOCIATED WAVE PROPAGATION PROBLEM

EDWARD I-HO LIN[†] and JEROME L. SACKMAN

Department of Civil Engineering, University of California, Berkeley, CA 94721, U.S.A.

(Received 3 June 1974)

Abstract—A method is developed for the identification of the dynamic properties of nonlinear viscoelastic materials using transient response information arising from impact tests. The solutions of the identification problem and that of the associated nonlinear wave propagation problem are shown to be coupled. They are accomplished via application of the method of lines, the Runge-Kutta-Pouzet integration scheme with automatic step size control and Powell's method of unconstrained optimization. Numerical experiments are performed to demonstrate the feasibility, accuracy and stability of the solution procedure established, and wave propagation experiments are conducted to investigate the applicability of the method to a real physical system. The results are of particular interest in the modeling of nonlinear viscoelastic materials and the identification of systems governed by nonlinear hyperbolic partial-integro-differential equations.

INTRODUCTION

The recent developments of constitutive theories in continuum mechanics have resulted in many highly complicated functional relations characterizing material behavior. The practical application of these sophisticated constitutive models has been restricted by the lack of knowledge of parameters or functions appearing in the functional relations on the one hand, and by the difficulty associated with the solution of the resulting nonlinear boundary (or initial-boundary) value problems on the other. Numerical methods for solving the direct problem (i.e. the boundary or initial-boundary value problem) have been extensively studied, and some of them, e.g. the finite element method, have emerged as very powerful tools. The inverse problem of determining the unknown parameters or functions characterizing the materials via realistic information (e.g. experimental data), however, has been less developed by researchers in the field, although the importance of this problem has been emphasized and solution methods investigated in recent years by Sackman and Kaya[1] Distefano[2,3], Distefano and Pister[4], Pister[5], etc.

In[1], Sackman and Kaya laid down the analytical bases for the direct determination of the short-time portion of creep and relaxation functions of linear viscoelastic materials, utilizing measurement of a response quantity at two different locations in the medium, or measurements of two different response quantities at the same location. Kaya carried out some numerical and experimental studies in his dissertation[6] following[1]. Considering a similar linear viscoelastic constitutive relation, as in[1], but assuming data to be available in the form of stress-strain pairs, Distefano[2] formulated the identification problem in such a way that creep and relaxation functions can be obtained by methods of differential approximation and quasilinearization. Reference[3] extends[2] to the consideration of a nonlinear viscoelastic constitutive relation in the same spirit, but substitutes a Gauss-Newton iterative scheme for quasilinearization. Other works using similar methods as in[2] and [3] include[4] and[7]. While the treatment of identification problems in the realm of the mechanics of continua is fairly recent, a large amount of earlier and current publications on system identification can be found in connection with system analysis and adaptive control problems. The recent monograph of Phillipson[8] treats the state identification problem of linear distributed systems, and that of Sage and Melsa[9] examines many of the existing techniques for system identification, with emphasis placed on parameter identification. Many important references on the subject can be found in these two books.

We consider in this paper a class of nonlinear viscoelastic materials whose constitutive equation is given by a certain nonlinear Volterra integral equation. By means of the procedure

[†]Currently, Assistant Mechanical Engineer, Argonne National Laboratory, Argonne, Illinois.

developed hereinafter, the unknown functions appearing in this equation are identified utilizing transient response measurements at several stations of the medium. The solution of the identification (or inverse) problem is shown to be coupled with that of the associated wave propagation problem, i.e. the prediction (or direct) problem. The feasibility, accuracy and stability of the procedure are demonstrated by numerical experiments performed using both uncorrupted and noisy data, and the applicability of the procedure to real physical systems is demonstrated by wave propagation experiments conducted on a polyethylene specimen. The need both of a realistic constitutive theory and of a sound identification algorithm for practical modeling is stressed.

It should be noted that in the realm of system identification, treatment of problems involving partial differential equations has been scarce. The usual treatments have been concerned mostly with systems governed by ordinary differential equations, and, as pointed out by Angel[10], methods devised for these systems are generally not suitable for distributed systems. Our method here, however, is applicable to systems governed by nonlinear partial differential as well as partial integro-differential equations.

FORMULATION OF THE PROBLEM

Consider longitudinal wave propagation in a circular cylindrical rod which is initially quiescent and which is composed of a homogeneous nonlinear viscoelastic material whose constitutive equation is given by the following nonlinear Volterra integral equation

$$\sigma(t) = K(O)G(\epsilon(t)) + \int_0^t G(\epsilon(\tau))K'(t - \tau)d\tau \quad (1)$$

where σ and ϵ denote the longitudinal stress and strain, respectively, t is the time. K and G are material functions and a prime indicates the derivative of a function. It is assumed that the effects of lateral inertia and shear can be neglected and that plane cross-sections remain plane. It is further assumed that the length of the rod is such as to guarantee that reflected waves would not arrive at the observation stations during the time period of interest. Thus, during the finite time interval $[O, T]$, we consider only the first passage of longitudinal waves travelling down the rod. The equation of motion is taken to be

$$\frac{\partial \sigma}{\partial x} = \rho \frac{\partial^2 u}{\partial t^2} \quad (2)$$

where ρ denotes the density of the rod, assumed constant everywhere, u the longitudinal displacement and x the longitudinal spatial coordinate. K and G in eqn (1) are functions assumed to be continuous, with K at least once differentiable.

Differentiating eqn (2) with respect to x , and making use of the relation $\epsilon = \partial u / \partial x$ (valid for small strains) we get

$$\frac{\partial^2 \sigma}{\partial x^2} = \rho \frac{\partial^2 \epsilon}{\partial t^2} \quad (3)$$

Differentiating eqn (1) twice with respect to x , and combining the results with eqn (3), we obtain

$$\begin{aligned} \rho \frac{\partial^2 \epsilon}{\partial t^2} = K(O) \left[G'(\epsilon) \frac{\partial^2 \epsilon}{\partial x^2} + G''(\epsilon) \left(\frac{\partial \epsilon}{\partial x} \right)^2 \right] \\ + \int_0^t \left[G'(\epsilon) \frac{\partial^2 \epsilon}{\partial x^2} + G''(\epsilon) \left(\frac{\partial \epsilon}{\partial x} \right)^2 \right] K'(t - \tau) d\tau \end{aligned} \quad (4)$$

where ϵ and its partial derivatives are functions of x and t outside the integral sign and functions of x and τ under the integral sign. Equation (4) is a nonlinear hyperbolic integro-differential equation of the Volterra type which governs the longitudinal wave propagation phenomenon in the rod.

Now suppose that strain histories are measured at three stations \bar{x}_1 , \bar{x}_2 , and \bar{x}_3 along the rod,

designated $\bar{\epsilon}_1(t)$, $\bar{\epsilon}_2(t)$ and $\bar{\epsilon}_3(t)$, respectively, where $0 \leq t \leq T$. The problem we wish to solve is: Based on these strain measurements, to identify the functions $G(\epsilon)$ and $K(t)$ in eqn (1), and to predict strain histories at other stations of the rod.

THE SOLUTION OF A NONLINEAR WAVE EQUATION

In order to solve the problem posed above, let us first consider solving eqn (4) in the rectangle $0 \leq t \leq T$, $x_L \leq x \leq x_R$ subject to the initial conditions

$$\epsilon(x, 0) = \frac{\partial \epsilon}{\partial t}(x, 0) = 0, \quad x_L \leq x \leq x_R \quad (5)$$

and the boundary conditions

$$\begin{aligned} \epsilon(x_L, t) &= \bar{\epsilon}_L(t), \quad 0 \leq t \leq T \\ \epsilon(x_R, t) &= \bar{\epsilon}_R(t), \quad 0 \leq t \leq T \end{aligned} \quad (6)$$

where $\bar{\epsilon}_L(t)$ and $\bar{\epsilon}_R(t)$ are the known strain histories at the left and right boundaries, respectively. Supposing that the functions $K(t)$ and $G(\epsilon)$ in eqn (4) are known, one way to obtain the numerical solution to eqns (4)–(6) is by first applying the method of lines [11] to eqn (4), thus approximating it by a system of nonlinear ordinary Volterra integro-differential equations, and then integrating this resulting system by the Runge–Kutta–Pouzet scheme [12] equipped with an automatic step size control mechanism [13] (see [14] and, for recent application of the method of lines, [15] and [16]).

Specifically, to apply the method of lines, we draw a set of straight lines $x = x_k \equiv x_L + kh$ parallel to the t -axis in the rectangle, where $k = 0, 1, 2, \dots, N + 1$, and $h = (x_R - x_L)/(N + 1)$. Let $\epsilon_k(t)$ be the approximation of $\epsilon(x_k, t)$ on the straight line $x = x_k$ and replace the spatial derivatives in eqn (4) by the following difference expressions

$$\begin{aligned} \frac{\partial^2 \epsilon}{\partial x^2}(x_k, t) &\approx \frac{1}{h^2} [\epsilon_{k+1}(t) - 2\epsilon_k(t) + \epsilon_{k-1}(t)] \\ \frac{\partial \epsilon}{\partial x}(x_k, t) &\approx \frac{1}{2h} [\epsilon_{k+1}(t) - \epsilon_{k-1}(t)] \end{aligned} \quad (7)$$

Such approximations are of $O(h^2)$ and are valid only if the solution to eqns (4)–(6) is sufficiently smooth. This substitution results in the following system of nonlinear Volterra integro-differential equations:

$$\begin{aligned} \rho \frac{d^2 \epsilon_i}{dt^2} &= \frac{K(O)}{h^2} [G'(\epsilon_i)(\epsilon_{i-1} - 2\epsilon_i + \epsilon_{i+1}) + \frac{1}{4} G''(\epsilon_i)(\epsilon_{i-1} - \epsilon_{i+1})^2] \\ &+ \frac{1}{h^2} \int_0^t [G'(\epsilon_i)(\epsilon_{i-1} - 2\epsilon_i + \epsilon_{i+1}) + \frac{1}{4} G''(\epsilon_i)(\epsilon_{i-1} - \epsilon_{i+1})^2] K'(t - \tau) d\tau, \quad (8) \\ &i = 1, 2, \dots, N; \quad 0 \leq t \leq T, \end{aligned}$$

where $\epsilon_0 = \bar{\epsilon}_L$ and $\epsilon_{N+1} = \bar{\epsilon}_R$, which follow from the boundary conditions (6).

We can readily convert eqn (8) to a system of first order equations which, together with the initial conditions (5) reads:

$$\begin{aligned} \frac{d\epsilon_i}{dt} &= \xi_i(t) \\ \frac{d\xi_i}{dt} &= \frac{K(O)}{\rho h^2} [G'(\epsilon_i)(\epsilon_{i-1} - 2\epsilon_i + \epsilon_{i+1}) + \frac{1}{4} G''(\epsilon_i)(\epsilon_{i-1} - \epsilon_{i+1})^2] \\ &+ \frac{1}{\rho h^2} \int_0^t [G'(\epsilon_i)(\epsilon_{i-1} - 2\epsilon_i + \epsilon_{i+1}) + \frac{1}{4} G''(\epsilon_i)(\epsilon_{i-1} - \epsilon_{i+1})^2] K'(t - \tau) d\tau, \\ &i = 1, 2, \dots, N; \quad 0 \leq t \leq T \end{aligned}$$

with

$$\epsilon_i(O) = \xi_i(O) = O, i = 1, 2, \dots, N. \quad (10)$$

We then integrate eqn (9) with initial conditions (10) numerically by the Runge-Kutta-Pouzet scheme with automatic step size control. The solution of eqns (4)–(6) by this method has been successfully carried out in [14]; the results compare favorably with wave propagation experiments and, in cases where the wave equation is linear, with those obtained by other numerical methods.

THE SOLUTION OF THE IDENTIFICATION AND PREDICTION PROBLEM

Recall that $\bar{\epsilon}_1(t)$, $\bar{\epsilon}_2(t)$ and $\bar{\epsilon}_3(t)$ are the measured strain histories at stations \bar{x}_1 , \bar{x}_2 and \bar{x}_3 of the rod, respectively. We observe that for the portion of the rod which occupies $[\bar{x}_1, \bar{x}_3] \subset R$ (the real line), $\bar{\epsilon}_1(t)$ and $\bar{\epsilon}_3(t)$ are nothing but the boundary conditions on the two ends. Since the rod is quiescent at $t = 0$, we have an initial-boundary value problem exactly like that represented by eqns (4)–(6), provided that $G(\epsilon)$ and $K(t)$ in eqn (4) are given certain definite specifications. This direct problem can be solved quite accurately for $\epsilon(x, t)$ in the rectangle $\bar{x}_1 \leq x \leq \bar{x}_3$, $0 \leq t \leq T$ by the method described above; in particular, it can be solved for $\epsilon(\bar{x}_2, t)$, $0 \leq t \leq T$. Clearly, if $G(\epsilon)$ and $K(t)$ were given the correct specifications, we would certainly expect $\epsilon(\bar{x}_2, t)$ to be in good agreement with $\bar{\epsilon}_2(t)$.

In more precise terms, we may state that the identification problem is to find the best $G(\epsilon)$ and $K(t)$ so as to bring $\epsilon(\bar{x}_2, t)$ as close to $\bar{\epsilon}_2(t)$ as possible. For a measure of closeness, the L_2 -norm appears to be a natural choice; note that generally (based on physical experience) there is no difficulty in realizing the square-integrability of $\epsilon(\bar{x}_2, t)$ and $\bar{\epsilon}_2(t)$, or for that matter, of any function appearing in eqn (4). However, since both $\bar{\epsilon}_2(t)$ (experimental data) and $\epsilon(\bar{x}_2, t)$ (calculated by the computer) are usually given by their values at discrete time points, it seems sensible to define the L_2 -norm on a finite point set

$$X = \{t_i | t_i \in [0, T], i = 1, 2, \dots, M\}$$

rather than on the continuous interval $[0, T]$. Thus the distance between $\epsilon(\bar{x}_2, t)$ and $\bar{\epsilon}_2(t)$ is given by $\|\epsilon(\bar{x}_2, t) - \bar{\epsilon}_2(t)\|_{L_2(X)}$ or, equivalently, by

$$\sum_{i=1}^M [\epsilon(\bar{x}_2, t_i) - \bar{\epsilon}_2(t_i)]^2 \quad (11)$$

This, in fact, is the well-known least squares distance function. Weights may be inserted in the above sum, as is sometimes done, to reflect the varying importance of particular data.

Now, considering the functions $G(\epsilon)$ and $K(t)$, let it be assumed that $G(\epsilon)$ is continuous, and thus admits the approximation (by virtue of the Weierstrass approximation theorem [17])

$$G(\epsilon) \approx \sum_{i=1}^m a_i \epsilon^i \quad (12)$$

Also, since $K(t)$ is similar to a relaxation function, a customary representation is here adopted.

$$K(t) \approx \sum_{i=1}^n b_i e^{-c_i t} \quad (13)$$

Thus, if $P \equiv \{a_0, \dots, a_m, b_0, \dots, b_n, c_0, \dots, c_n\}$ then the identification problem is to find the best P so that the sum of squares (11) attains its minimum value. Since $\epsilon(\bar{x}_2, t_i)$ is defined by the solution of eqns (4)–(6) which depends on the parameters P , the problem can be explicitly stated as

$$\min_P \left(\sum_{i=1}^M [\epsilon(\bar{x}_2, t_i; P) - \bar{\epsilon}_2(t_i)]^2 \right) \quad (14)$$

It must be pointed out that at this stage very little is known about the parameters P , hence no

constraints can be explicitly imposed on them. Equations (4)–(6) are unquestionably a constraint on the state $\epsilon(\bar{x}_2, t; P)$, but they can be considered as a constraint on the parameters only to the extent that P must be such that the equations are soluble. As long as the equations are soluble the parameters P should be able to enjoy complete freedom. Unfortunately, at the moment, there is hardly any nontrivial information available as to what P will not permit a solution of eqns (4)–(6). If the minimization problem (14) is to be treated as a constrained problem, with eqns (4)–(6) serving as constraints, then the Lagrange multiplier technique may be employed, and the adjoint equations have to be solved (see [9] for simpler examples). However, due to the complexity of eqns (4)–(6), and of their approximation by eqns (9)–(10), it is desirable to avoid dealing with additional equations such as the adjoint equations. We therefore choose to treat (14) as an unconstrained minimization problem with eqns (4)–(6) serving to define the objective function rather than as constraints. Thus it is implicitly assumed that no constraints exist among the parameters, which in turn implies that they are linearly independent. Generally they would be so only if the approximating forms for $G(\epsilon)$ and $K(t)$ are chosen properly. In practice, not knowing the constraints even when they do exist may require more initial guesses of the parameter values to be tried, but hopefully some understanding of the physical situation, and intuition, will lead to reasonable initial estimates of the parameters.

In selecting an efficient algorithm to deal with this unconstrained minimization problem, considerations are given to: (i) The objective function in (14) assumes the form of a sum of squares, i.e. (14) is a least squares minimization problem; (ii) The objective function (in particular, $\epsilon(\bar{x}_2, t; P)$ in eqn (14)) is defined by the solution of the nonlinear hyperbolic integro-differential equation (4) with initial boundary conditions given by eqns (5) and (6), and obtaining a numerical solution by means of a computer is rather time consuming. Thus it is highly desirable to limit the number of times that these equations have to be solved; (iii) If gradients of the objective function are required, their exact evaluations would require solutions of equations similar to eqns (4)–(6), and computing time is again a serious problem. Therefore, it will be advantageous if ways can be found to avoid exact evaluation of the gradients, i.e. to avoid computation of the derivatives. One of the few efficient algorithms currently available which fulfills all these considerations is that of Powell. A detailed description of this algorithm can be found in [18] or [14]; the latter publication also examines the suitability of the method of quasilinearization for the present problem.

Using Powell's algorithm, the minimization problem (14) can be successfully carried out, as will be shown by results presented in the sequel. Thus, the best parameters P will be found which, in turn, will determine the best $G(\epsilon)$ and $K(t)$ via eqns (12) and (13), and the solution of eqns (4)–(6) at $x = \bar{x}_2$ will be in the closest agreement with experimental measurement at that station, in the sense of the L_2 -norm defined or, equivalently, in the least squares sense. With the functions $G(\epsilon)$ and $K(t)$ so identified, a prediction of $\epsilon(x, t)$ for $x \in [\bar{x}_1, l]$ and $0 \leq t \leq T$ can be readily obtained by solving eqns (4)–(6), using for the left boundary condition the strain history measured at $x = \bar{x}_1$, and using for the right boundary condition zero at $x = l' > l$; how much bigger l' should be than l depends on how close $x = l$ is to the position x where $\epsilon(x, t)$ is wanted and how big the time interval of interest $[0, T]$ is, the idea being to eliminate at the position x of interest, reflections coming from the end $x = l'$.

It should be noted that the above procedure for solving the identification and prediction problem can still be executed even if strain measurements were only made at two stations, say \bar{x}_1 and \bar{x}_2 . In this case, the right boundary condition would be taken as zero at some \bar{x}_3 located sufficiently far away from \bar{x}_2 . Obviously, the bigger the interval $[\bar{x}_1, \bar{x}_3]$, the more computational work will be required; on the other hand, \bar{x}_1 , \bar{x}_2 and \bar{x}_3 should be sufficiently far apart so that measurements made at these stations may, by means of the differences among them that reflect the evolution of the disturbance as it travels in the system, embody rich enough information to effect a good solution of the problem. These are points to be heeded during the design of the experiments. Also, if more than three measurements are made, say four at \bar{x}_a , \bar{x}_b , \bar{x}_c and \bar{x}_d , then measurements at \bar{x}_a and \bar{x}_d can be taken as boundary conditions, and those at \bar{x}_b and \bar{x}_c can be used in an expression similar to that in expression (11) as the distance function.

An alternative solution involving a system of ordinary differential equations instead of one of integro-differential equations is possible, if $K(t)$ is to be approximated by the sum of exponentials (13). This is demonstrated for simple cases in [14], where very good results were

obtained. However, such formulations generally require higher order numerical differentiation of experimental data, which is usually to be avoided.

NUMERICAL EXPERIMENTATION

In order to demonstrate the feasibility, accuracy and stability of the solution procedure previously described, several numerical experiments were performed using both uncorrupted and noisy data for the nonlinear viscoelastic material considered above. Experiments for linear viscoelastic and nonlinear elastic materials were also conducted and satisfactory results obtained. Only results for the nonlinear viscoelastic material are presented in the following; those for linear viscoelastic and nonlinear elastic materials can be found in [14].

Case 1. Uncorrupted data

Consider a circular cylindrical rod of unit length whose constitutive model is given by eqn (1) or, more specifically, by

$$\sigma(t) = K(O) G(\epsilon(t)) + \int_0^t G(\epsilon(\tau)) K'(t - \tau) d\tau$$

$$G(\epsilon) = \epsilon + B_1 \epsilon^3, \quad K(t) = B_2 - \frac{B_3}{B_4} (1 - e^{-B_4 t}) \quad (20)$$

To generate numerical data, we solved eqns (4), (5) and (6) with $x_L = 0$, $x_R = 1$, $T = 0.25$.

$$\bar{\epsilon}_l(t) = \begin{cases} \sin^2 8\pi t & 0 \leq t \leq 0.125 \\ 0 & 0.125 \leq t \leq 0.25 \end{cases}$$

$$\bar{\epsilon}_R(t) = 0 \quad 0 \leq t \leq 0.25$$

and with values of the parameters B_1 , B_2 , B_3 and B_4 given as "exact value" in Table 1. The density ρ was taken to be 1 for convenience. In applying the method of lines, we took $h = 0.05$, i.e. the rod was divided into 20 "elements." Solutions at 19 stations $x = 0.05i$, $i = 1, 2, \dots, 19$, were recorded, and they constituted the numerical data $\bar{\epsilon}_i(t)$. Figure 1 shows some of the generated strain histories $\bar{\epsilon}_5(t)$, $\bar{\epsilon}_8(t)$ and $\bar{\epsilon}_{11}(t)$.

For identification, values of the parameters were then considered to be unknown, and the data $\bar{\epsilon}_5(t)$, $\bar{\epsilon}_8(t)$ and $\bar{\epsilon}_{11}(t)$ were used for their determination; the identification procedure described earlier was used to this end. Values of the parameters at different stages of iteration are given in Table 1, and the corresponding predictions of the strain history at station 8 are shown in Fig. 2. It is seen from Table 1 that the final identified values of B_1 and B_2 agree quite well with their exact values, and although the final values of B_3 and B_4 do not match as well with the exact values, the strain prediction at the 6th iteration (Fig. 2) is already hardly distinguishable from the data.

A prediction of the strain at all stations was then carried out using the identified parameter values and employing $\bar{\epsilon}_8(t)$ as input. Strain predictions at stations 6 and 9 are shown in Fig. 3, where their good correlation with the data is evident.

Table 1. Results of parameter identification—Case 1

Iteration	Parameter Value				Squared Deviation ($\times 10^{-4}$)
	B_1	$B_2 (\times 10^{10})$	$B_3 (\times 10^{10})$	B_4	
1 (Initial Guess)	0.20000	0.17100	0.45000	4.50000	9892.27
2	-0.42134	0.14135	0.08497	11.0799	2.13426
11 (Converged)*	-0.50000	0.14077	0.03920	10.6163	0.13698
Exact Value	-0.50000	0.14000	0.85000	8.00000	

*Convergence is taken to be reached if each parameter changes by less than 10^{-5} times its value.

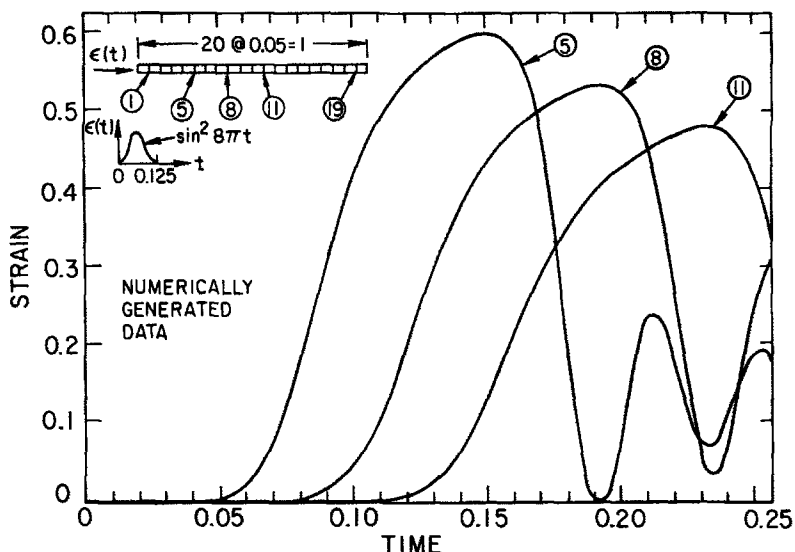


Fig. 1. Numerically generated strain histories—Case I.

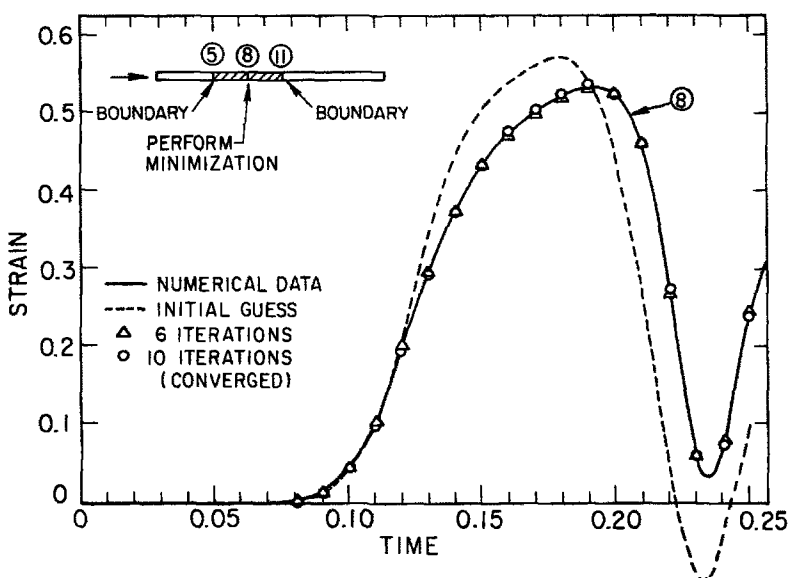


Fig. 2. Pulse prediction at various stages of identification—Case I.

In this case, the integration of the system of nonlinear Volterra integro-differential equations was performed using a third order Runge-Kutta-Pouzet scheme. A time step $\Delta t = 0.000625$ was used, and the total effective computing time (central processor time plus a prescribed fraction of peripheral processor time) for identification and prediction on a CDC 6400 digital computer was 286 seconds.

Case II. Noisy data

The numerical data generated in Case I were corrupted artificially by using the noise model

$$\epsilon_c(t) = [(1 + e)\eta + (1 - e)(1 - \eta)]\epsilon(t)$$

where $e = 0.05$ (5% noise) was used, and η , a normalized pseudo-random variable uniformly distributed on $[0,1]$, was generated by an existing subroutine, so that the noise model can also be written as

$$\epsilon_c(t) = (0.95 + 0.1\eta)\epsilon(t).$$

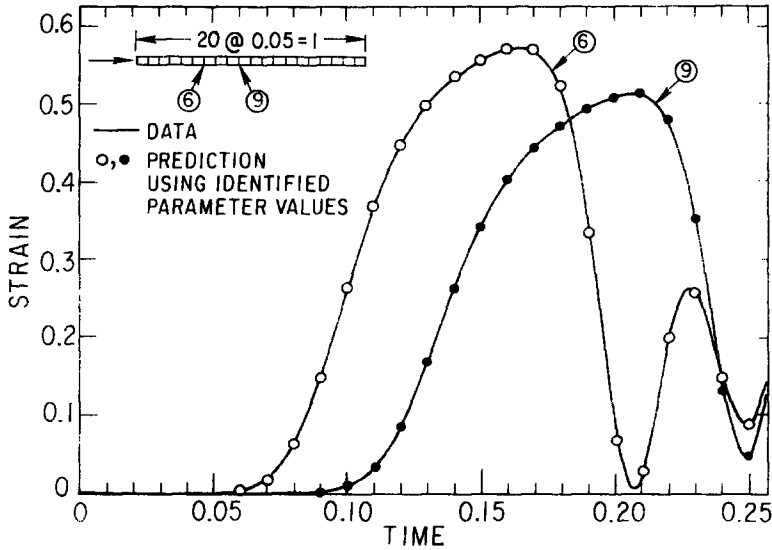


Fig. 3. Pulse prediction after identification is completed—Case I

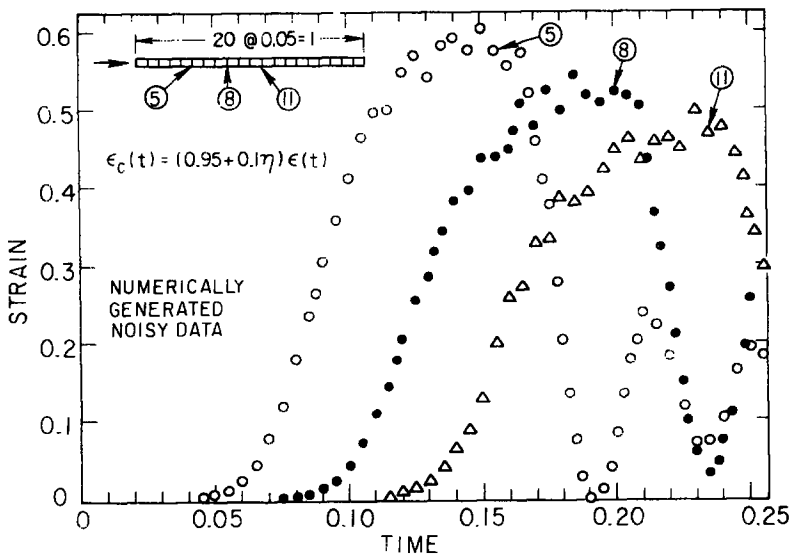


Fig. 4. Numerically generated noisy strain histories—Case II.

Figure 4 shows the noisy strain data at stations 5, 8 and 11.

These data were then used for identification. Values of the parameters at different stages of iteration are given in Table 2, and the corresponding predictions of strain at station 8 are shown in Fig. 5. A comparison between Tables 1 and 2 as well as Figs. 2 and 5 shows that, although more iterations are required for convergence in the noisy case, the final results in this case are no worse than those in the uncorrupted case; B_1 , the coefficient of the nonlinear term, is seen to be affected most by the noise. It is worth noting that, contrary to common expectation, no difficulty of any kind arose due to the presence of noise.

Prediction of strain at stations 6 and 9 using parameter values identified by the noisy data was executed and compared in Fig. 6 with uncorrupted data generated in Case I. Agreement is excellent; in fact, very little distinction can be made between Figs. 3 and 6. In this case, a third order Runge-Kutta-Pouzet integration scheme and a time step $\Delta t = 0.000625$ were used throughout, and the total effective computing time for identification and prediction was 431 seconds.

Table 2. Results of parameter identification—Case II

Iteration	Parameter Value				Squared Deviation ($\times 10^{-2}$)
	B_1	$B_2(\times 10^{10})$	$B_3(\times 10^{10})$	B_4	
0 (Initial Guess)	0.20000	0.17100	0.45000	4.50000	75.6904
8	-0.52483	0.18179	1.03208	14.4459	0.81209
15 (Converged)	-0.52471	0.17961	0.91909	10.6136	0.73405
Exact Value	-0.50000	0.18000	0.85000	8.00000	

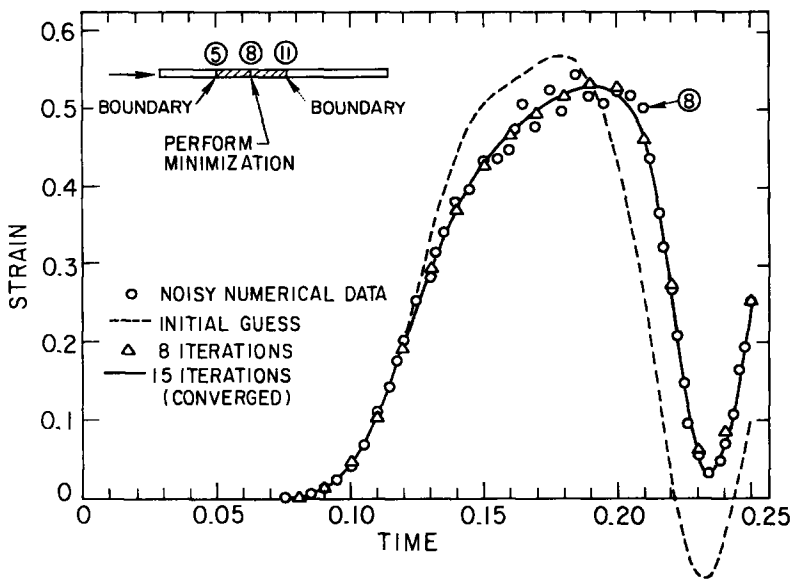


Fig. 5. Pulse prediction at various stages of identification—Case II.

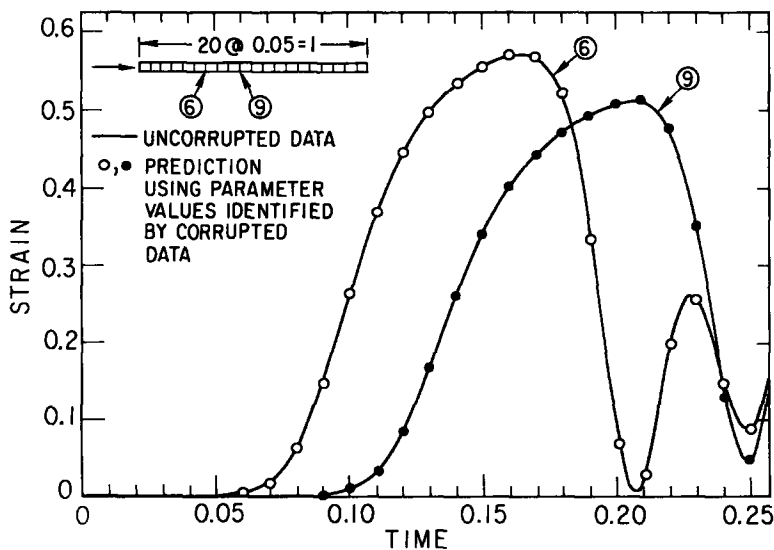


Fig. 6. Pulse prediction after identification is completed—Case II.

Case III. Uncorrupted data generated by a model different from the proposed model

Instead of using the constitutive model (20) to generate numerical data, we used in this case a different model, i.e.

$$\begin{aligned} \sigma(t) &= J(O)F(\epsilon(t)) + \int_0^t H(\epsilon(\tau))J'(t-\tau)d\tau \\ F(\epsilon) &= 1 - e^{-0.65\epsilon}, H(\epsilon) = 1 - e^{-0.74\epsilon} \\ J(O) &= 22.5 \times 10^8, J'(t) = -60 \times 10^8 e^{-8t} - 9 \times 10^8 e^{-2.7t} \end{aligned} \tag{21}$$

In other words, in order to obtain data, the following equation was solved subject to the same boundary and initial conditions as in Case I:

$$\begin{aligned} \rho \frac{\partial^2 \epsilon}{\partial t^2} &= J(O) \left[F'(\epsilon) \frac{\partial^2 \epsilon}{\partial x^2} + F''(\epsilon) \left(\frac{\partial \epsilon}{\partial x} \right)^2 \right] \\ &+ \int_0^t \left[H'(\epsilon) \frac{\partial^2 \epsilon}{\partial x^2} + H''(\epsilon) \left(\frac{\partial \epsilon}{\partial x} \right)^2 \right] J'(t-\tau) d\tau \end{aligned}$$

where ρ was again taken to be 1 for convenience. Figure 7 shows the generated strain histories at stations 5, 8 and 11.

Now despite the fact that these data are generated by using model (21), we proposed to identify the material using model (20). The results of parameter identification are shown in Table 3, and the corresponding predictions of strain at station 8 are shown in Fig. 8.

Predictions of strain at stations 6 and 9 based on identified model (20) were then executed and compared with data generated based on model (21) in Fig. 9. The agreement between predictions

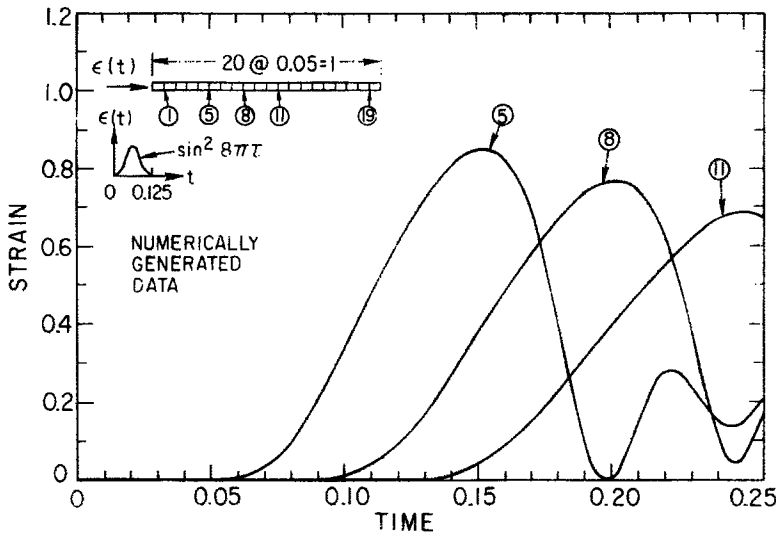


Fig. 7. Numerically generated strain histories—Case III.

Table 3. Results of parameter identification—Case III

Iteration	Parameter Value				Squared Deviation ($\times 10^{-2}$)
	B_1	$B_2 (\times 10^{10})$	$B_3 (\times 10^{10})$	β_d	
0 (Initial Guess)	-0.50000	0.18000	0.85000	2.50000	102.084
7	-0.17148	0.13014	0.74809	16.6655	1.25706
13 (Converged)	-0.18077	0.13288	0.86997	20.2734	0.11277

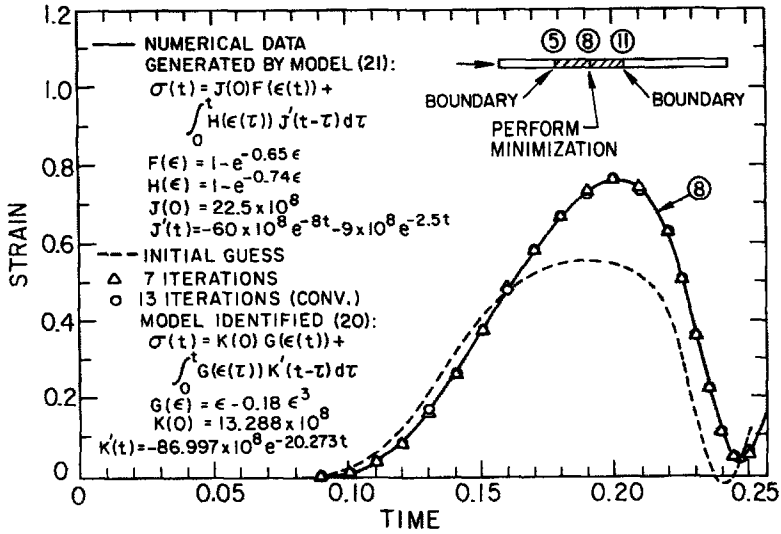


Fig. 8. Pulse prediction at various stages of identification—Case III.

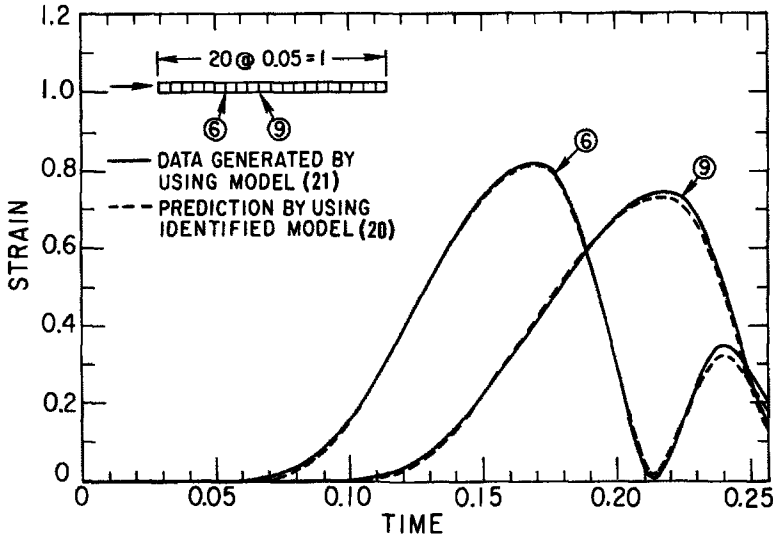


Fig. 9. Pulse prediction after identification is completed—Case III.

and data as shown in Figs. 8 and 9 is quite remarkable, considering the fact that they are based on two completely different models.

On one hand, this demonstrates the non-uniqueness of model representation with respect to a certain specific purpose, i.e. for a certain intended use, there may be several different but equivalent models suitable for a given physical system. On the other hand, this strengthens the hope of acquiring a decent model (useful, but not too complicated) for any given system, because this example shows that even if the “real model” should be model (21), model (20) does provide a decent approximation. Furthermore, the fact that one exponential term for $K'(t)$ in model (20) is adequate to take the place of two exponential terms for $J'(t)$ in model (21) suggests that the inclusion of more exponential terms in the usual relaxation or creep function may not always be substantially helpful, but may only increase the burden of computation in many cases.

The integration scheme and time step used here were the same as in Cases I and II. The total effective computing time for identification and prediction in this case was 448 seconds.

NONLINEAR VISCOELASTIC WAVES IN POLYETHYLENE AND THE CHARACTERIZATION OF ITS DYNAMIC PROPERTIES

Having established the feasibility, accuracy and stability of the solution method by the numerical experiments presented above (and in [14]), we proceed to demonstrate the applicability

of the method to a real physical system. The Hopkinson pressure-bar technique was employed to perform wave propagation experiments on a circular cylindrical polyethylene bar, $\frac{1}{2}$ in. in diameter and approximately 3 ft in length with specific gravity equal to 0.896. Upon impact by a projectile (steel ball) on the end of the bar, a pulse was generated and propagated down the specimen, on which strain gauges were attached to record the passage of the pulse. Figure 10 presents the recorded strain histories at four different stations of the bar. (A full account of the experimental details can be found in [14].) The metamorphosis of the transient as well as the diminution of its amplitude is evident, the later being attributed largely to the viscoelasticity of the material.

In order to carry out the identification procedure, a constitutive model for the material used has to be first hypothesized. It should be emphasized that, in general, if the chosen model is inadequate to portray the given system, then any identification attempt would be futile; in other words, a realistic constitutive model and a sound identification algorithm are both essential in accomplishing a meaningful and useful characterization of the material properties. In conducting numerical experiments with an identification algorithm to ascertain its feasibility, accuracy and stability, one seeks to be assured of the soundness of the algorithm; thus when an identification attempt fails to yield expected results, one may turn to alternative representations of the constitutive model. In the present case, the constitutive model (20) was tried, and the results turned out to be quite satisfactory. Following the previously described procedure, the strain histories measured at stations 5 and 1 (Fig. 10) were taken to be the boundary conditions of the bar segment 5-1, quiescent initial conditions were imposed, the parameter values were guessed, the strain history at station 3 was predicted, and an objective function consisting of the sum of squared deviations of this predicted strain history from the measured strain history at station 3 was minimized to yield values of the parameters B_1 , B_2 , B_3 and B_4 in (20). The values of these parameters at different stages of iteration are given in Table 4, while the corresponding predictions of strain at station 3 are shown in Fig. 11. Convergence of iteration was taken to be achieved when each parameter changed by less than 10^{-5} times its value. As can be seen from Table 4, the parameter values at the fifth iteration were quite close to their final values, and from Fig. 11, both the final parameter values and those at the fifth iteration yielded fairly good predictions for the pulse at station 3. In fact, the results of the fifth iteration seemed even better as far as agreement of peak values was concerned (though the twelfth iteration was better in the least squares sense). In the identification process, a third order Runge-Kutta-Pouzet integration scheme, $\Delta x = 1$ in. (i.e. the bar segment 5-1 was divided into 12 elements), and $\Delta t = 0.0025$ msec were used throughout; the total effective computing time was 596 sec.

Since peak amplitude is important for practical purposes, the parameter values obtained at the fifth iteration were used next to predict the strain history at station 4 (which had not been used in the identification process) as well as at other stations. To this end, the experimental data at station

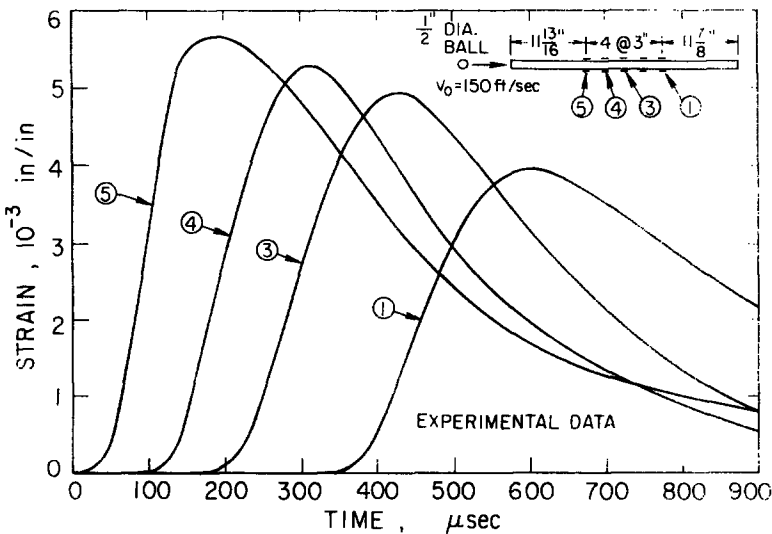


Fig. 10. Longitudinal strain histories due to impact by a $\frac{1}{2}$ -in-dia steel ball

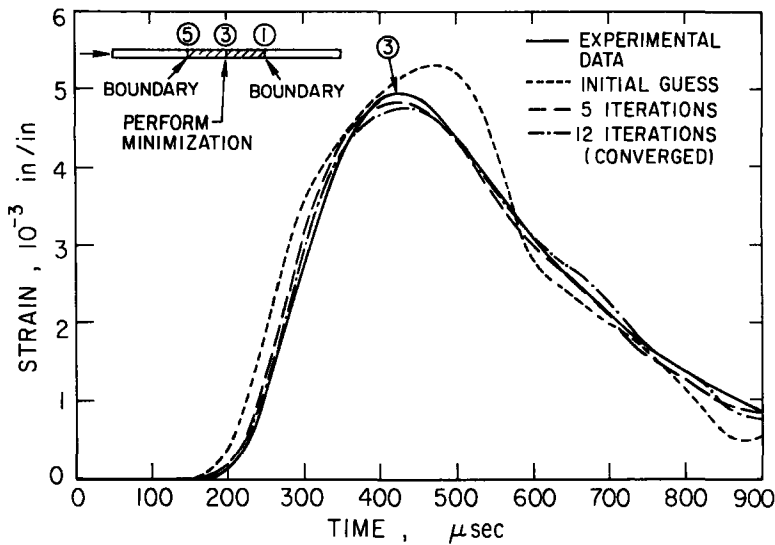


Fig. 11. Pulse prediction at various stages of identification.

Table 4. Dynamic characterization of polyethylene based on the experimental data (Fig. 10)

Iteration	Parameter Value				Squared Deviation ($\times 10^{-5}$)
	$B_1 (\times 10^4)$	$B_2 (\times 10^5)$ $1b/in^2$	$B_3 (\times 10^6)$ $1b/in^2/msec$	B_4 $1/msec$	
0 (Initial Guess)	-0.71000	1.25000	0.40000	16.5030	1.48650
5	-0.54910	0.98624	0.12961	0.66049	0.19099
12 (Converged)	-0.59517	0.95702	0.12620	0.49606	0.10153

3rd order Runge-Kutta-Pouzet scheme
 $\Delta x = 1$ in; $\Delta t = 0.0025$ msec
 Total effective computing time = 596 sec

*Convergence is taken to be reached if each parameter changes by less than 10^{-5} times its value.

5 were used as the left boundary condition, and the right boundary condition was taken to be zero at a station 2 ft.-5 in. to the right of station 5. (Such a distance was chosen to make sure that reflections from the right boundary would not arrive at station 1 within 900 μ sec.). The results of the prediction are shown in Fig. 12 by the dashed line. Very good agreement with the data was obtained except for the rear portion of the pulse at station 1.

To see if such a nonlinear identification was really necessary, i.e. to see if a linear identification could not have produced equally good results, the same experimental data were used in IDENTIF[19], a program written for identification of linear viscoelastic materials based on [1]. Such linear identification required only data from two stations, so that an identification was made based on data at stations 5 and 3, and stations 5 and 1, respectively. This resulted in creep functions as shown in Fig. 13, which also includes a 5-parameter least-squares exponential fit to the averaged creep function obtained by means of the computer program FITEXP [20]. The 5-parameter exponential fit was further used for prediction by means of PREDICT, a companion program of IDENTIF written on the basis of [21]. The prediction results are presented in Fig. 12 where comparison can be made with nonlinear prediction. It is evident that the nonlinear prediction was superior to the linear prediction. It is of interest to note that $B_1 = -0.59517 \times 10^4$ indicates a nonlinearity effect of almost 20% at the maximum strain level of 5.67600×10^{-3} in/in.

CONCLUSION

A method for solving an identification-prediction problem has been presented along with several numerical experiments demonstrating its feasibility, accuracy and stability: its applicabil-

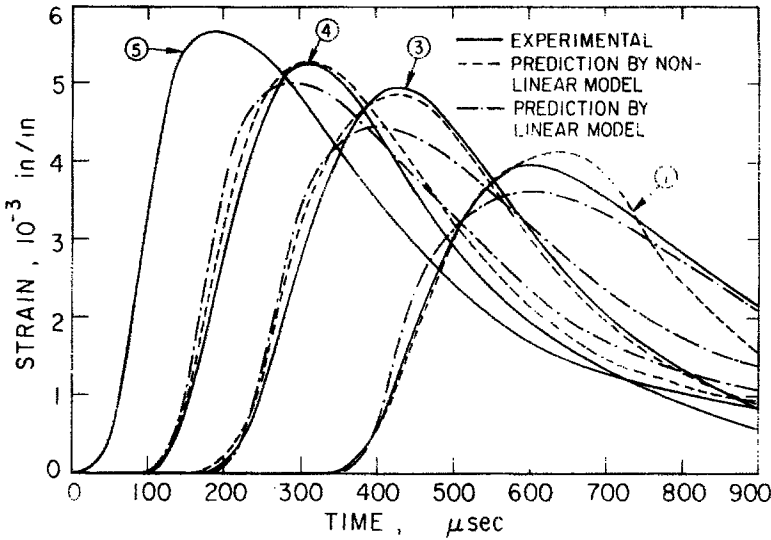


Fig. 12. Pulse prediction after identification is completed

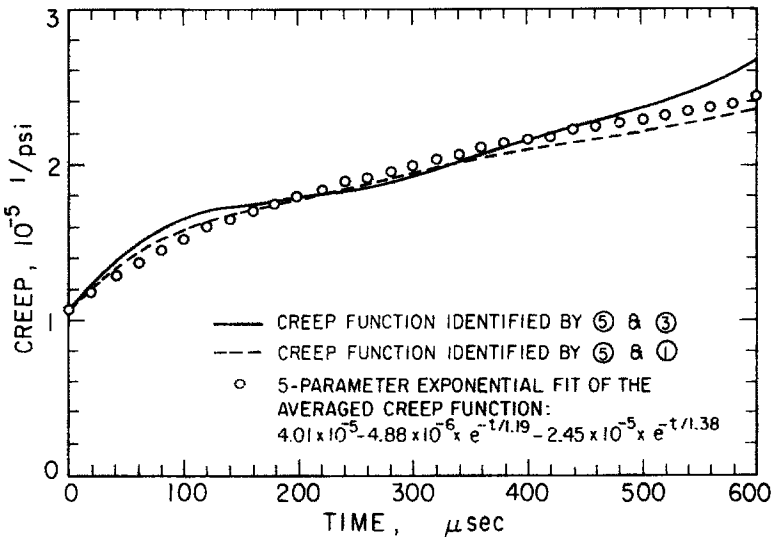


Fig. 13. Creep functions from linear identification.

ity to real physical systems was investigated by wave propagation experiments conducted on a polyethylene specimen. Although demonstrated only for a particular class of nonlinear viscoelastic materials, the method can be applied to nonlinear elastic and linear viscoelastic materials with equal success [14]. In fact, it seems obvious that the method should be applicable to many more physical problems of the identification-prediction type. The extension of the method to three-dimensional problems also appears, in principle, to be straightforward if the method of lines is used to discretize three, instead of one, spatial axis, or, equivalently, if a finite element discretization is employed. It should be noted that the formulation in terms of stress or particle velocity can also be easily effected.

As the choice of proper constitutive models is difficult in dealing with real materials, the practitioner may find some consolation in the results of Case III above, where it was possible to employ a simple model (which was sufficiently rich) to suitably characterize a behavior which was in actuality more complex than that contained in the simple model used in the identification procedure. The results of the experimental investigation of polyethylene bars show that our method is applicable to real materials. The characterization arrived at, however, should not be taken as complete: whether the model identified on the basis of data obtained from experiments involving a certain input regime is sufficient to predict the material response for inputs in a

completely different regime remains to be verified. This touches upon the question of the "domain of applicability" of an identified model, which is briefly discussed in [14] and which remains an important but, so far, unresolved problem in the field of identification.

Acknowledgements—The authors gratefully acknowledge the partial support of this research by the Lawrence Livermore Laboratory, the National Science Foundation, and the University of California, Berkeley.

REFERENCES

1. J. L. Sackman and I. Kaya, On the determination of very early-time viscoelastic properties. *J. Mech. Phys. Solids* **16**, 121 (1968).
2. N. Distéfano, On the identification problem in linear viscoelasticity. *ZAMM* **50**, 638 (1970).
3. N. Distéfano, Some numerical aspects in the identification of a class of nonlinear viscoelastic materials. *ZAMM* **52**, 389 (1972).
4. N. Distéfano and K. S. Pister, On the identification problem for thermorheologically simple materials. *Acta Mechanica* **13**, 179 (1972).
5. K. S. Pister, Mathematical modeling for structural analysis and design. *Nuclear Eng. and Design* **18**, 353 (1972).
6. I. Kaya, Very early time characteristics of linear viscoelastic materials. *Ph.D. dissertation*, University of California, Berkeley (1968).
7. N. Distéfano and R. Todeschini, Modeling, identification and prediction of a class of nonlinear viscoelastic materials. *Int. J. Solids Struct.* **9**, 805 (1973).
8. G. A. Phillipson, *Identification of Distributed Systems*. American Elsevier, New York (1971).
9. A. P. Sage and J. L. Melsa, *System Identification*. Academic Press, New York (1971).
10. E. Angel, Inverse boundary-value problem: elliptic equations. *J. Math. Anal. Appl.* **30**, 86 (1970).
11. I. S. Berezin and N. P. Zhidkov, *Computing Methods*. Vol. II, (Translation by O. M. Blunn) Pergamon Press, Oxford (1965).
12. P. Pouzet, Méthode d'intégration numériques des équations intégrales et integrodifferentielles du type Volterra de seconde espèce. Formules de Runge-Kutta. *Proc. Rome Symposium on the numerical treatment of ordinary differential equations, integral and integro-differential equations* pp. 362-368 Birkhäuser Verlag, Basel (1960).
13. J. A. Zonneveld, *Automatic Numerical Integration*. Mathematical Center Tracts 8, Amsterdam (1964).
14. I. H. Lin and J. L. Sackman, On identification and prediction of dynamical systems governed by nonlinear hyperbolic integro-differential equations of Volterra type. *SESM Report 73-15* University of California, Berkeley (Dec. 1973).
15. J. S. Hicks and J. Wei, Numerical solution of parabolic partial differential equations with two-point boundary conditions by use of the method of lines. *J. ACM* **14**, 549 (1967).
16. A. Zafarullah, Application of the method of lines to parabolic partial differential equations with error estimates. *J. ACM* **17**, 294 (1970).
17. I. Stakgold, *Boundary Value Problems of Mathematical Physics*. Vol. I. Macmillan, New York (1967).
18. M. J. D. Powell, A method for minimizing a sum of squares of nonlinear functions without calculating derivatives. *Computer J.* **7**, 303 (1965).
19. J. L. Sackman, C. L. Wu and G. N. Owen Jr., *User's manual for the digital computer program IDENTIF*. University of California, Berkeley (1969).
20. R. Taylor, Private communication, University of California, Berkeley.
21. J. L. Sackman and I. Kaya, On the propagation of transient pulses in linearly viscoelastic media. *J. Mech. Phys. Solids* **16**, 346 (1968).